Large Evaporite Provinces: Geothermal rather than Solar Origin?

Zhanjie Qin
Chinese Academy of Sciences
Chunan Tang (catang@mechsoft.cn)
Dalian University of Technology
Xiying Zhang
Chinese Academy of Sciences
Tiantian Chen
Northeastern University
Xiangjun Liu
Northwest Normal University
Yongshou Li
Chinese Academy of Sciences
Zhen Chen
Sun Yat-Sen University
Lianting Jiang
South China Sea Institute of Oceanology, Chinese Academy of Sciences

Article

Keywords: Large evaporite provinces (LEPs), evaporites, salt deposits, evaporitic basins

Posted Date: October 8th, 2020

DOI: https://doi.org/10.21203/rs.3.rs-80284/v2

Large Evaporite Provinces: Geothermal rather than Solar Origin?

Z.J. Qin[1,2], C.A. Tang[3,4]*, T.T. Chen[5], X.J. Liu[6], Y.S. Li[1,2], Z. Chen[7], L.T. Jiang[8], X.Y. Zhang[1,2]

[1]Key Laboratory of Comprehensive and Highly Efficient Utilization of Salt Lake Resources, Qinghai Institute of Salt Lakes, Chinese Academy of Sciences, Xining 810008, China
[2]Qinghai Provincial Key Laboratory of Geology and Environment of Salt Lakes, Xining 810008, China
[3] State Key Laboratory of Coastal & Offshore Engineering, Dalian University of Technology, Dalian 116024, China
[4] State Key Laboratory of Geological Processes and Mineral Resources, China University of Geosciences (Wuhan) 430074, China
[5]School of Resources and Civil Engineering, Northeastern University, Shenyang 110819, China
[6]College of Geography and Environmental Science, Northwest Normal University, Lanzhou 730070, China
[7]School of Earth Sciences and Geological Engineering, Sun Yat-sen University, Guangzhou 510275, China
[8]Key Laboratory of Ocean and Marginal Sea Geology, South China Sea Institute of Oceanology, Chinese Academy of Sciences, Guangzhou 510301, China

*Correspondence to: tca@mail.neu.edu.cn

Large evaporite provinces (LEPs) represent prodigious volumes of evaporites widely developed from the Sinian to Neogene. The reasons why they often quickly develop on a large scale with large areas and thicknesses remain enigmatic. Possible causes range from warming from above to heating from below. The fact that the salt deposits in most salt-bearing basins occur mainly in the Sinian-Cambrian, Permian-Triassic, Jurassic-Cretaceous, and Miocene intervals favours a dominantly tectonic origin rather than a solar driving mechanism. Here, we analysed the spatio-temporal distribution of evaporites based on 138 evaporitic basins and found that throughout the Phanerozoiceon, LEPs occurred across the Earth's surface in most salt-bearing basins, especially in areas with an evolutionary history of strong tectonic activity. The masses of evaporites, rates of evaporite formation, tectonic movements, and large igneous provinces (LIPs) synergistically developed in the Sinian-Cambrian, Permian, Jurassic-Cretaceous, and Miocene intervals, which are considered to be four of the warmest times since the Sinian. We realize that salt accumulation can proceed without solar energy and can generally be linked to geothermal changes in tectonically active zones. When climatic factors are involved, they may be manifestations of the thermal influence of the crust on the surface.

The traditional definition of evaporite is a chemically precipitated salt generally containing carbonate, sulphate and chloride salts formed on the basis of their own saturability in concentrated brine in a certain tectonic environment[1]. Under this paradigm, concentrated brine was usually considered to be the result of evaporation of natural water by the solar energy. For example, the "Bar theory"[2], "Desert-basin theory"[3], and "Deep-water theory"[4], etc., were the classical salt-forming theories of seawater by evaporation of solar. However, the origin of salt giants thousands of metres thick in marine environments are difficult to decipher by these traditional models[5,6], e.g. the large evaporite deposits in the Mediterranean (~3 km in thickness), Red Sea (>3 km in thickness) and Atlantic (>2 km in thickness)[7,8,9,10]. These salt giants were usually accumulated in active tectonic environments (subduction or rift) and accompanied by some magmatic-hydrothermal events, which may occur as parts of "Wilson cycles"[5,6]. Meanwhile, the complicated hydrodynamics, thermodynamics and properties of brines and the processes of solid-liquid phase transformations in these salt giants were different from the traditional salt formation models[5,6,9,10,11]. The current upsurge in the study of evaporite dynamics, the development of new evaporite mechanisms and the ensuing controversies[5,6,8,9,10,11] have led to re-assessment of various roles in salt accumulation. Therefore, a new systematic salt accumulation mechanism is eagerly needed for these large salt deposits.

Throughout the Phanerozoic, a total of 138 evaporitic basins were collected around the world (Fig. 1 and Extended Data Table 1). Among them, 21 basins (15%) were on stable craton blocks, 50 basins (36%) were in convergent subduction tectonic settings, and 66 basins (49%) were in rifting environment. These evaporitic basins developed episodically, mainly in the Precambrian-Cambrian, Permian, Jurassic-Cretaceous, and Miocene periods (Fig. 2a). The Precambrian and early Palaeozoic intervals were characterized by cratonic basins, convergent basins were dominant in the Cambrian and Cenozoic, and rift basins were mainly distributed in the Mesozoic (Fig. 2a). In addition, the masses of evaporites (halite) were different in three types of tectonic basins through geological time[12]. The evaporite mass was less than 4000×10^{15} kg (average 924×10^{15} kg) in all cratonic basins, while the maximum was approximately$11{,}000\times10^{15}$ kg (average 2343×10^{15} kg) in subduction settings and rift basins (Fig. 2b, c). Specifically, large amounts of halite was accumulated on the ocean floor, such as ~8400×10^{15} kg in the Gulf of Mexico in the Jurassic, ~6000×10^{15} kg on the seabed of the North and South Atlantic in the Cretaceous, and ~2300×10^{15} kg on the sea floor of the Mediterranean and Red Seas in the Miocene[12]. These data indicated that the ocean floor, as subduction or rifting environments, was in favour of salt formation in seawater. Moreover, the rates of salt formation in different tectonic basins were calculated from statistical data (Extended Data Table 4). The rate of salt formation in cratonic basins ranged from ~0.02×10^{15} kg/Ma to ~70×10^{15} kg/Ma (average ~19×10^{15} kg/Ma), while it ranged from ~0.9×10^{15} kg/Ma to ~290×10^{15} kg/Ma (average ~73×10^{15} kg/Ma) in subduction settings and rift basins. For example, the rates of salt accumulation on the sea floor of the Mediterranean and Red Seas in the Miocene, the North and South Atlantic in the Cretaceous, and the Gulf of Mexico in the Jurassic were ~134×10^{15} kg/Ma , ~76×10^{15} kg/Ma and ~156×10^{15} kg/Ma, respectively (Fig. 2d). Accordingly, the masses and salt-forming rates of evaporite in different tectonic basins demonstrated that salt giants were more easily accumulated in active tectonic environments than in stable cratons. This might be related to the geothermal properties of subduction and rifting tectonic environments in specific geological time, which were usually the breeding grounds of magmatic events and hydrothermal activity.

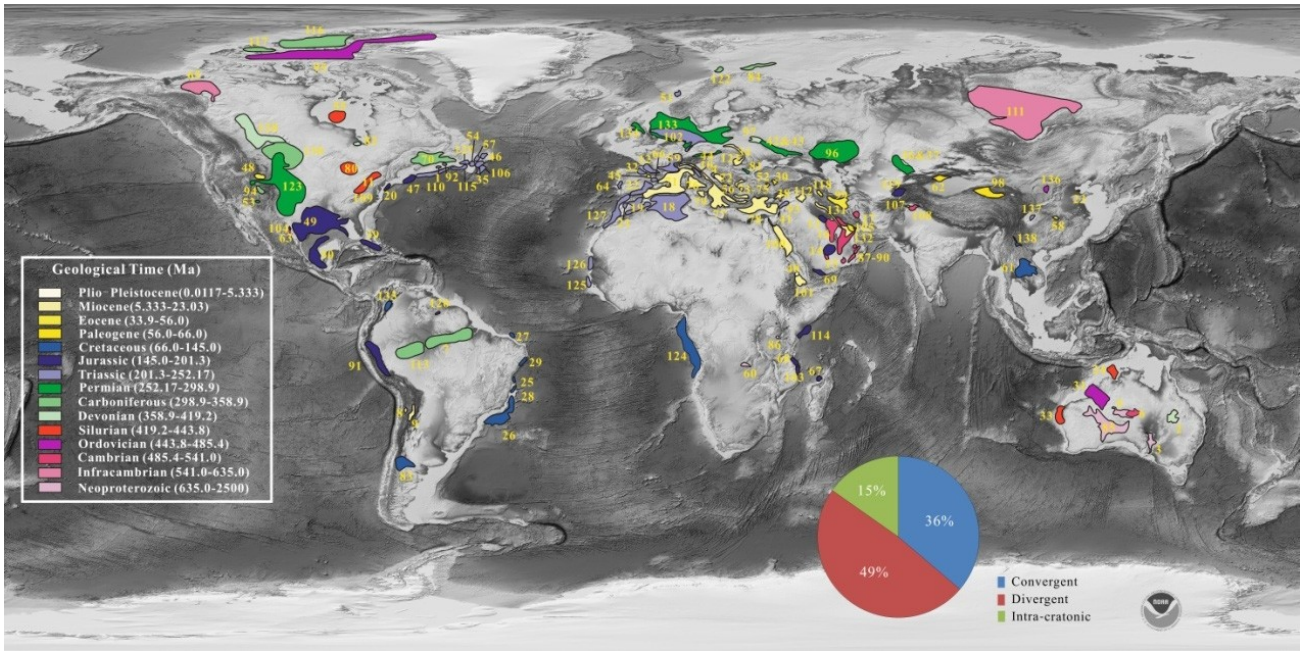

Fig.1 | Distribution of evaporitic basins around the world through geological time (redrawn from[1,25]) (Extended Data Table 1). Basin names: 1. Abenaki (N. Scotian), 2. Adavale, 3. Adelaide Fold Belt, 4. Adriatic-Albanian Foredeep, 5. Amadeus Basin, 6. Amadeus Basin (Chandler), 7. Amazonas, 8. Andean, 9. Andean, 10. Apennine, 11. Appalachian, 12. Aquitaine, 13. Arabian Basin (Gotnia Salt Basin), 14. Arabian Basin (Hith Salt Basin), 15. Arabian Basin (Hormuz central Saudi Arabia), 16. Arabian Basin (Hormuz Gulf region), 17. Arabian Basin (Hormuz-Kerman region), 18. Atlas (Algerian-Tunisian), 19. Atlas (Moroccan), 20. Baltimore Canyon, 21. Berrechid, 22. Betic-Guadalquivir Basin, 23. Bohai Basin, 24. Bonaparte (Petrel), 25. Brazilian Aptian Basin (Camamu), 26. Brazilian Aptian Basin (Campos-Santos), 27. Brazilian Aptian Basin (Ceara), 28. Brazilian Aptian Basin (Cumuruxatiba), 29. Brazilian Aptian Basin (Sergipe-Alagoas), 30. Cankiri-Corum, 31. Canning Basin, 32. Cantabrian-West Pyrenees, 33. Carnarvon Basin (Yaringa), 34. Carpathian foredeep, 35. Carson Basin (Grand Banks), 36. Chu-Sarysu (Devonian), 37. Chu-Sarysu (Permian), 38. Cicilia-Latakia, 39. Cuban, 40. Danakil, 41. Dead Sea, 42. Dniepr-Donets, 43. Dniepr-Donets, 44. Eastern Alps, 45. Ebro Basin, 46. Flemish Pass Basin (Grand Banks), 47. Georges Bank, 48. Green River Basin, 49. Gulf of Mexico (northern Gulf coast), 50. Gulf of Mexico (southern; Salina-Sigsbee), 51. Haltenbanken, 52. Haymana-Polatli, 53. Holbrook Basin, 54. Horseshoe Basin (Grand Banks), 55. Hudson Bay, 56. Ionian, 57. Jeanne d' Arc Basin (Grand Banks), 58. Jianghan Basin, 59. Jura/Rhodanian, 60. Katangan, 61. Khorat Basin, 62. Kuqaforeland (Tarim Basin), 63. La Popa (Monterrey) Basin, 64. Lusitanian, 65. Mackenzie Basin, 66. Maestrat, 67. Majunga Basin, 68. Mandawa Basin, 69. Ma' Rib-Al Jawf/Shabwah (Hadramaut), 70. Maritimes Basin, 71. Mediterranean-Western, 72. Mediterranean-Adriatic, 73. Mediterranean-Andros Basin, 74. Mediterranean-Cretean Basin, 75. Mediterranean-Samothraki basin, 76. Mediterranean-Tyrrhenian, 77. Mediterranean-Central, 78. Mediterranean-Eastern, 79. Mediterranean-Sicilian, 80. Michigan Basin, 81. Moesian, 82. Moose River Basin, 83. Neuquen Basin, 84. Nordkapp Basin, 85. Officer Basin, 86. Olduvai depression, 87. Oman (Fahud Salt Basin), 88. Oman (Ghaba Salt Basin), 89. Oman (Ghudun Salt Basin), 90. Oman (South Oman Salt Basin), 91. Oriente-Ucayali (Pucara) Basin, 92. Orpheus Graben, 93. Palmyra, 94. Paradox Basin, 95. Parry Island Fold Belt, 96. Pricaspian Basin, 97. Pripyat Basin, 98. Qaidam Basin, 99. Qom-Kalut, 100. Red Sea (north), 101. Red Sea (south), 102. Rot Salt Basin, 103. Ruvuma Basin, 104. Sabinas Basin, 105. Sachun Basin, 106. Salar Basin (Grand Banks), 107. Salt Range (Hormuz-Punjab region), 108. Salt Range (Kohat Plateau), 109. Saltville (Appalachian), 110. Scotian Basin, 111. Siberia, East, 112. Sirjan Trough,113. Solimoes, 114. Somalia-Kenya, 115. South Whale Basin (Grand Banks), 116. Sverdrup Basin (EllefRingnes-NW Ellesmere), 117. Sverdrup Basin (Melville Is.), 118. Tabriz Salt Basin, 119. Tadjik Basin, 120. Takutu Salt Basin, 121. Transylvanian, 122. Tromso Basin, 123. USA Midcontinent, 124. West Africa (Angola-Gabon), 125. West Africa (Gambia-Guine Bissau), 126. West Africa (Mauritania-Senegal), 127. West Africa (Morocco-S.Spain), 128. Western Canada (Alberta Basin), 129. Whale Basin (Grand Banks), 130. Williston Basin, 131. Zagros (Mesopotamian Basin), 132. Zagros (Mesopotamian Basin), 133. Zechstein (NW Europe), 134. Zechstein (onshore UK), 135. Zipaquira Basin, 136. Erdos Basin, 137. Sichuan Basin, 138. Lanping-Simao Basin.

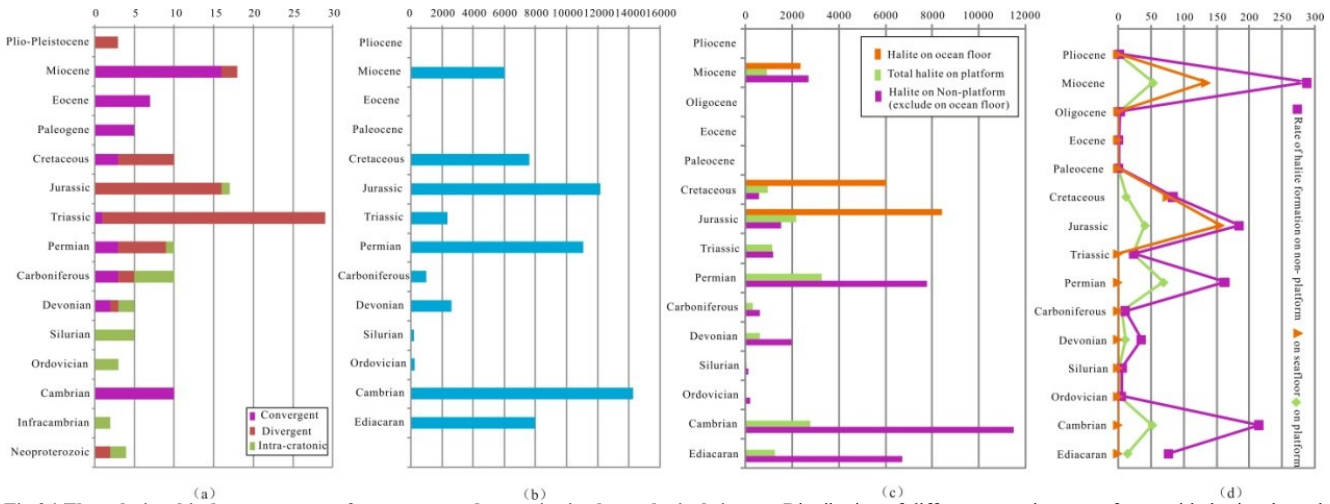

Fig.2 | The relationship between mass of evaporate and tectonics in the geological time. a, Distribution of different tectonic types of evaporitic basins through geological time (data from[1]). **b,** Total masses of halite in different geological periods(mass×10^{15} kg).**c,** Masses of halite in different tectonic types of evaporitic basins through geological time (mass×10^{15} kg). **d,** Rates of salt formation in different tectonic types of evaporitic basins through geological time (10^{15} kg/Ma); (data are from[12, 26, 27]).

To reveal the inter-relationships between evaporite and geothermal events in active tectonic settings around the world, the salt giant with a mass of halite >2000×10^{15} kg and a rate of salt formation >70×10^{15} kg/Ma is preliminarily defined as a large evaporite province (LEP) based on the tectonic types of the basin, masses of evaporite, and rates of salt formation. For instance, the East Siberian evaporite province in the Cambrian, Zechstein evaporite province in the Permian, Gulf of Mexico evaporite province in the Jurassic, Atlantic evaporite province in the Cretaceous and Mediterranean and Middle East evaporite provinces in the Miocene can be considered as the LEPs. During four main salt-forming geological times, we compared the LEPs with the Large Igneous Provinces (LIPs), an extreme magmatic thermal event, and found that the LIPs were always accompanied by the LEPs (Fig. 3). In detail the LIPs of

European-Northwest African (EUNWA)/Skagerrak (~300 Ma), the Central Atlantic magmatic province (CAMP) (~201 Ma), the Paraná-Etendeka (~132 Ma), the Afro-Arabra (~30 Ma), and the Pan-Mediterranean (~6.0 Ma) occurred in association with the Zechstein LEP in the late Permian[14], the Gulf of Mexico LEP in the Middle Jurassic[15], the South Atlantic LEP in the Middle Cretaceous[16], the Red Sea and the Mediterranean LEPs in the Miocene[17], respectively (Extended Data Table 5). The LIP is a mainly mafic magmatic province with an areal extent >0.1 Mkm^2 and an igneous volume >0.1 Mkm^3. It usually has intraplate characteristics and is often emplaced in a short duration pulse or multiple pulses (less than 1-5 Ma) with a maximum duration of<~*c*.50 Ma[18]. In spite of the intervals between the LIPs and LEPs, there might be positively promoting effect to accumulation of the LEPs from the LIPs. Recently, Hovland et al.[5,6] suggested a model of large salt accumulation based on hydrothermal processes within Wilson cycles and proposed that solid salt was easily formed in subduction and rifting tectonic environments, such as the Andean subduction zone (oceanic-continental subduction), the Mediterranean ridge subduction zone (oceanic-oceanic subduction), and the East African and Rea Sea rifts. This is consistent with our analysis of statistic data of distributions, masses, and salt-forming rates of evaporite deposits in the world. Sternai et al.[22] also found that the formation of the Messinian salinity crisis (MSC) in the Mediterranean was associated with volcanic activity (igneous rock) and considered that the MSC promoted the production and eruption of magma. However, the heat and denser brines produced by magma activity might also contribute to the formation of the MSC, and the potential heat transfer between brines and magmas could not be concluded exactly.

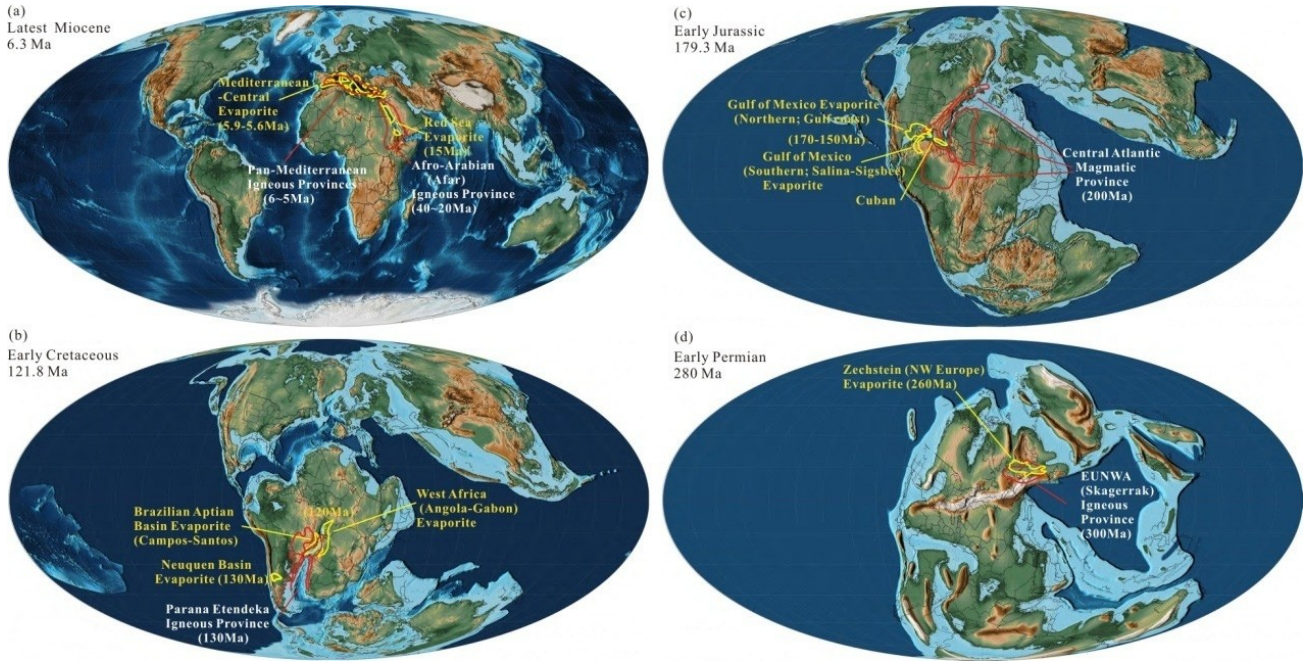

Fig.3 | Comparisons between Large Igneous Provinces (LIPs) (data are from[18]), and Large Evaporite Provinces (LEPs) (data are from[12,26,27]) in different tectonic settings through the geological time (data are from[28,29]). a-d show the corresponding relationships of locations and ages. a. The Pan-Mediterranean igneous province and the Mediterranean evaporite, and the Afro-Arabian igneous province and the Red Sea evaporite in the Miocene; b. the Parana Etendeka igneous province and the South Atlantic evaporite in the Cretaceous; c. the Central Atlantic Magmatic Province and the Gulf of Mexico evaporite in the Jurassic; d. the Eunwa igneous province and the Zechstein evaporite in the Permian.

Based on the discoveries of hot brines in the Atlantis II Deep of the Red Sea[19] and hot vents or 'black smokers' on the East Pacific Rise[20], Hovland et al.[5] inferred that 'forced convection' in seawater circulation is caused by the heat from the underlying mantle. In particular, concentrated brines and solid salt below the sea surface formed when the temperatures of the hydrothermally circulating seawater are greater than 400℃ and the sediment thickness is >3 km. In addition, these authors proposed that salt accumulation on the sea floor is associated with serpentinization of mantle rocks (peridotite) because mineral dissolution and hydrolysis in mantle rock were caused by seawater-rock exothermic interactions. This process resulted in significant releases of Cl^-, Mg^{2+}, and Na^+, which was favourable to formation of denser brines and/or solid salts[9,10,11]. Meanwhile, the accumulating process of salt from serpentinization was further verified by the theoretical calculation that 10.5 kg of salt will be produced by changing one m^3 of peridotite to serpentinite[21]. Therefore, this salt-forming phenomenon resulting from serpentinization might be a new model for the salt giant in the deep ocean. The coupling of heat of the magma, brines and complicated transforming process between water and salt in the subduction and rifting tectonic settings may be a perspective formation mechanism for the LEPs.

In fact, the Precambrian-Cambrian, Permian, Jurassic-Cretaceous, and Miocene were four of the warmest intervals since the Sinian. Very active geological events occurred during these periods, such as active orogenic belts, the break-up and assemblage of supercontinents, and changes in sea level, imply that they are not simply caused by climatic warming which cannot trigger such significant strong geological activity. The wide distribution of salt giants generally found in plate margins, deep oceanic basins in the Tethyan orogenic belt, transitional zones from sea to land, epicontinental seas and platform centres of isolated plates[13] also need a more reasonable explanation than climatic factors. Current ideas involve either the solar evaporite hypothesis that triggers salt accumulation by warming from above[1, 4, 24] or a hypothesis involving active lithospheric processes that provide heat from below[5, 6, 9, 10, 11]. At the least, from available evidence, researchers have realized that solar energy may not be the ultimate driving force for salt accumulation; that is, salt deposits can generally be linked to geothermal changes in plate boundaries and in the overall regime of plate tectonics, rather than solar energy. When climatic reasons are involved, they may have been manifestations of the thermal influence of the crust on the surface. Therefore, the LEPs may favour a dominantly tectonic origin rather than a solar evaporite theory. We believe that the LEPs formed in active tectonic settings are mainly controlled by heat from the upper lithospheric crust or mantle, which is obviously different from surficial evaporites controlled by solar evaporation.

But, what and how did the magmatic events happen and be controlled, which further influenced the formation and distribution of the LEPs in the geological time. Our recent studies on Earth's thermal evolution, as shown in Fig.4, suggest that Earth may experience extreme warming and cooling periods in terms of Earth's geothermal cycles[23]. The thermal expansion of the lithosphere induces uplift and then rifting, leading to the collapse of Earth's crust[30], with volcanism and magmatism as the global-scale response. This shallow process may reach a critical state with a positive feedback loop, resulting in LIPs, which may remove large amounts of heat from erupted lavas by radiation into the atmosphere. Endothermic phase changes during de-compressive melting also absorb large quantities of heat energy from Earth's interior, which cools their surroundings. This process may end a warming cycle and initiate a new cycle of climatic cooling, even a new ice age. To fully determine the exact geothermal cycles, one must determine all the starting point parameters and ingredients, as well as their evolution during the geologic processes. Of course, at the moment, reaching a very high degree of accuracy is not possible. Therefore, our model can only be regarded as a new perspective, and much more additional work has to be done to explain the details. However, if we accept the concept that the Earth evolves as a thermal system[23], it is natural to consider that over geological time spans, salts and brines may survive in the deep crust or mantle and that they may experience heat energy supply from several geological stages of the Wilson cycle before the salt clearly accumulated. The Earth has undergone several supercontinental cycles of assembly and break-up. The supply of heat energy and the availability of seawater during the long history of Earth's evolution make deep salt and brine production unavoidable. Therefore, the salt accumulations we observe today may be results of longer times than the latest stage in the Wilson cycle of thearea[5].

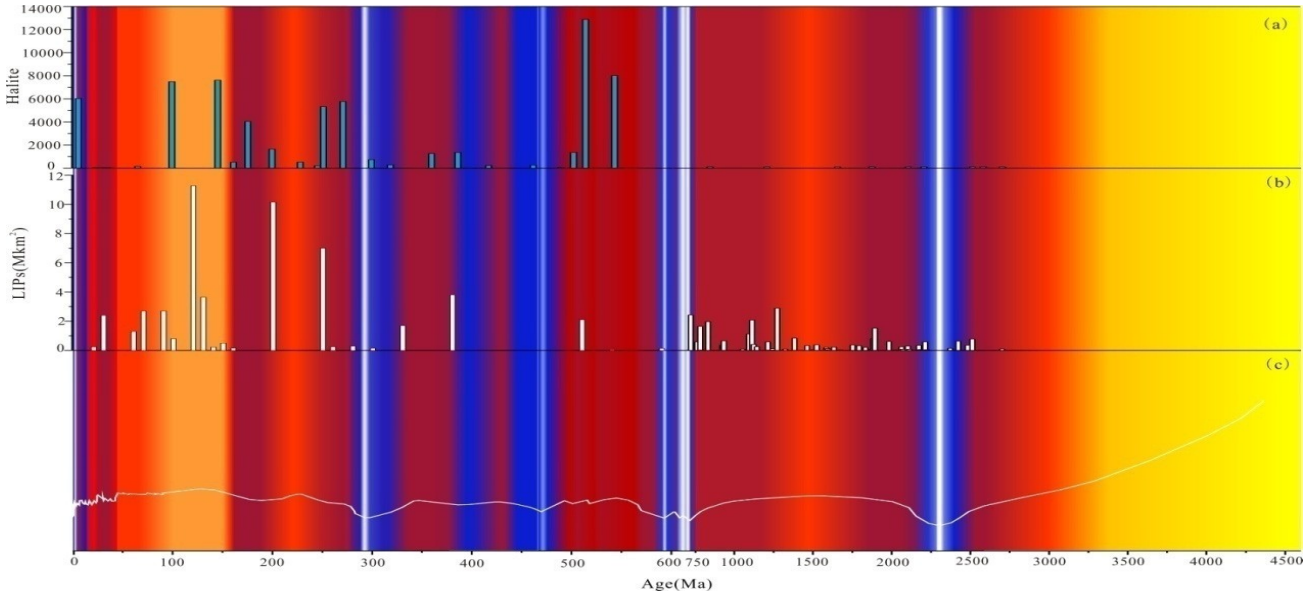

Fig.4 | The corresponding relationships among evaporate (halite), Large igneous provinces (LIPs) and Thermal cycle in the geological time (the colour in the figure indicates the relative temperature of Earth's surface layer, with yellow, red, blue and white representing temperature from warm to cool, respectively**). a,** Temporal distribution of masses of evaporites (redrawn from[12, 26, 27, 31-37]). **b,** Temporal distribution of area of the large igneous provinces (redrawn from[1, 18]). **c,** Schematic diagram of the global thermal cycle in Earth evolution (redrawn from[23]).

To all scientists in geology and geophysics who are familiar with solar evaporite theory, the debate about a solar or non-solar origin for LEPs is very thought- provoking. The profusion of LEPs in deep sea regions and the presence of canyons and magmatic provinces spatially related to the known LEPs suggest that the locations of LEPs, such as the Mediterranean Sea, could have been heated by large underlying shallow thermal anomalies rather than warmed by solar energy from above. A regional heat anomaly could be fed by deep-sourced heat accumulation incubating beneath the oceanic crust, with the heat unable to escape because of the crust's insulating effect. If this were true, the combination of changes in plate tectonic forces and uplift above a regional heat anomaly could have been sufficient to cause rifting and release enough heat energy to generate LEPs. We believe that hydrothermal processes may explain the locations and durations, as well as the amounts, of salt deposits in a better way than solar evaporation. However, as pointed out by Schreiber et al.[24], this interpretation does not exclude solar energy as one of the active contributors to brine densification and precipitation of solid salt in many cases.

Many debates concerning LEPs can be advanced only by improved imaging of geothermal regimes, which may lead to a better understanding of geodynamics. The questions of thermal anomalies in terms of their sizes, durations and distribution in the underlying mantle are very important and have to be answered. Further constraints on these hypotheses and models can also come with more precise dating of the relationships between thermal anomalies and the onset of LEPs by more clearly defining geothermal anomalies in large tectonic rifting and magmatic provinces and by exploring the thermal regime at the time of evaporite emplacement. Of most importance, however, is to achieve a better understanding of the whole platetectonic regime at the times of LEPs such as the MSC. In the future, geothermal evaporites will receive increasing attention. We will not be able to address the full picture of evaporites until we have a better understanding of Earth's thermal history[23]. If we can determine the meaning of and controls on LEPs formed during Earth's evolution history, we will be in a far better position to understand their mechanisms and assess the relative contributions of heat energy from above as a consequence of solar radiation or from below with deep mantle processes in a plate tectonic regime.

Reference:

1. Warren J.K. *Evaporites: a geological compendium, 2nd edn* (Springer International Publishing, Switzerland, 2016)
2. Ochsenius, C.C. *Die Bildung der Steinsalzlager und ihrer Mutterlangen Salze*. (Halle C. E. M. Pfeffer, Germany, 1877).
3. Walther, J. *Einleitung in die Geologie als historische Wissenschaft: Beobachtungen über die Bidung der Gesteine und ihrerorganischen Einschlüsse*. (Nabu Press, Germany, 1894).
4. Schmalz, R. F. Deep-water evaporite deposition: a genetic model. *AAPG Bull*. **53**, 798-823 (1969).
5. Hovland, M., Rueslatten, H., Johnsen, H. K. Large salt accumulations as a consequence of hydrothermal processes associated with 'Wilson cycles': A review Part 1: Towards a new understanding. *Mar. Petrol. Geol.* **92**, 987-1009 (2018a).
6. Hovland, M., Rueslatten, H., Johnsen, H. K. Large salt accumulations as a consequence of hydrothermal processes associated with 'Wilson cycles': A review Part 2: Application of a new salt-forming model on selected cases. *Mar. Petrol. Geol.* **92**, 128-148 (2018b).

7. Christeleit, E. C., Brandon, M. T., Zhuang, G. Evidence for deep-water deposition of abyssal Mediterranean evaporites during the Messinian salinity crisis. *Earth Planet Sci. Lett.* **427**, 226-235 (2015).
8. Lugli, S., Manzi, V., Roveri, M., Schreiber, B. C. The deep record of MEssinian salinity crisis: evidence of a non-desiccated Mediterranean Sea. *Palaeogeogr. Palaeoclimatol. Palaeoecol.* **433**, 201-218 (2015).
9. Scribano, V. et al. Origin of salt giants in abyssal serpentinite systems. *Int J Earth Sci*. **106**, 2595-2608(2017).
10. Scribano, V., Carbone, S., Manuella, F. C. Tracking the Serpentinite Feet of the Mediterranean Salt Giant. *Geosciences* **8**, 352 (2018).
11. Debure, M., Lassin, A., Marty, N. C., Claret, F., Virgone, A., Calassou, S., Gaucher, E. C. Thermodynamic evidence of giant salt deposit formation by serpentinization: an alternative mechanism to solar evaporation. *Sci Rep.* **9**, 11720 (2019).
12. Hay, W. W. et al. Evaporites and the salinity of the ocean during the Phanerozoic: Implications for climate, ocean circulation and life. *Palaeogeogr. Palaeoclimatol. Palaeoecol.* **240**, 3-46 (2006).
13. Li, J. H., Ma, L. Y., Wang, H. H., Xu, L. Geologic genesis and significance research of global saline giants. *Chin. J. Geol.* **51**, 619-632 (2016).
14. Hardie, L. A. The roles of rifting and hydrothermal $CaCl_2$ brines in the origin of potash evaporites, an hypothesis. *Am. J. Sci*. **290**, 43-106 (1990).
15. Ewing, W. M., Worzel, J. L., Burk, C. A. Regional aspects of deepwater drilling in the Gulf of Mexico, east of the Bahama Platform, and on the Bermuda Rise (eds Ewing, W. M.et al), *Initial Reports of the Deep Sea Drilling Project*. **1**, 624-640 (1969).
16. Davison, I. Geology and tectonics of the South Atlantic Brazilian salt basin. *Geol. Soc. London, Spec. Publ*. **272**, 345-359 (2007).
17. Mitchell, N. C., Ligi, M., Ferrante, V., Bonatti, E., Rutter, E. Submarine salt flows in the central Red Sea. *Geol. Soc. Am. Bull.* **122**, 701-713(2010).
18. Ernst, R. E. Large Igneous Provinces. (Cambridge University Press, Cambridge, 2014).
19. Charnock, H. Anomalous bottom water in the red sea. *Nature* **203**, 591 (1964).
20. Lonsdale, P., Clustering of suspension-feeding macrobenthos near abyssal hydrothermal vents at oceanic spreading centers. *Deep Sea Res*. **24**, 857-863(1977).
21. Scribano, V., Viccaro, M. En-route formation of silica-undersaturated melts through interaction between ascending basalt and serpentinite-related saline brines: inference from Hyblean Cenozoic nephelinites, Sicily. *Conference A. Rittmann At: Nicolosi (Ct), Italy Volume: Miscellanea* (INGV 25, 107, 2014).
22. Sternai, P.et al. Magmatic pulse driven by sea-level changes associated with the Messinian salinity crisis. *Nat. Geosci*. **10**,783-787(2017).
23. Tang, C. A., Li, S. Z. The Earth evolution as a thermal system. *Geol. J.* **51**, 652–668 (2016).
24. Schreiber, B.C., Lugli, S., Bąbel, M. *Evaporites Through Space and Time.* (The Geological Society London, London, 2007).
25. Liu, C. L. et al. Advance in the Study of Forming Condition and Prediction of Potash Deposits of Marine Basins in China's Small Blocks: Review. *Acta Geosci. Sin.* **37**, 581-606 (2016).
26. Floegel, S., Wold, C. N., and Hay, W. W. Evolution of sediments and ocean salinity. In *31st International Geological Congress*, 4, CD-ROM (IGC, 2000).
27. Gradstein, F. M., Ogg, J. G., Smith, A. G. et al. *A Geologic Time Scale*. (Cambridge University Press, Cambridge, 2004).
28. Haq, B. U., van Eysinga, F. W. B. *Geological TimeTable*, 5th Revised Edition. (Elsevier Science Publishers, Amsterdam, 1998).
29. Haq, B. U., Al-Qahtani, A. M. Phanerozoic cycles of sea-level change on the Arabian Platform. *Geo.Arabia*. **10**, 127-160 (2005).
30. Tang, C.A., Webb, A.A.G., Moore, W.B. et al. Breaking Earth's shell into a global plate network. *Nat. Commun.* **11**, 3621 (2020).

Methods:

In Fig. 2b, the masses of halite in different geological intervals are calculated by the following equation:

$$M_{TH}=M_{RH}+M_{OH}$$

where M_{TH} is the total mass of reconstructed halite on the Earth in different geological intervals, M_{RH} is the original recyclable halite mass reconstructed by the sum of total mass of recyclable halite and eroded halite since deposition and M_{OH} is the mass of halite on ocean floor (not recyclable). All the masses of halite are from the maximum estimates (i.e., Hay et al.[12]), because 1) the exploration of evaporites in the ocean basins and marginal seas is not sufficient to date and 2) many estimates of volumes and masses of halite in the deep sea are based on seismic data. However, future discoveries and corrections are unlikely to be large enough to invalidate the estimates. The reasonable assumptions and detailed calculation procedures for the masses of recyclable halite and eroded halite are from[12] (Extended Data Table 2). In Fig. 2c, the masses of halite on the ocean floor (M_{OH}) and platforms (M_{PH}) are calculated according to the data from [12, 26]. The masses of halite on non-platform areas (excluding the ocean floor) are calculated by M_{TH} minus M_{OH} and M_{PH} (Extended Data Table 3). In Fig. 2d, the rates of halite formation in different tectonic regimes (platform, non-platform excluding ocean floor, and ocean floor) are calculated by the ratios of total masses of halite to the length of age for halite formation (Extended Data Table 4). The equation is R=M/t.

Data availability:

31. Buick, R. The antiquity of oxygenic photosynthesis: evidence from stromatolites in sulphate-deficient Archaean lakes. Science 255, 74-77 (1992).
32. Eriksson, K. A., Simpson, E. L., Master, S., Henry, G. Neoarchaean (c. 2.58 Ga) halite casts: implications for palaeoceanic chemistry. J. Geol. Soc. 162, 789-799 (2005).
33. Gandin, A., Wright, D. T. Evidence of vanished evaporits in Neoarchaean carbonates of South Africa. Geol. Soc. London, Spec. Publ. 285, 285-308 (2007).
34. Kah, L. C., Lyons, T.W., Chesley, J. T. Geochemistry of a 1.2 Ga carbonate-evaporite succession, northern Baffin and Bylot Island: implications for Mesoproterozoic marine evolution. Precambrian Res. 111, 203-234 (2001).
35. Lindsay, J. F. Upper Proterozoic evaporites in the Amadeus Basin, central Australia, and their role in basin tectonics. Geol. Soc. Am. Bull. 99, 852-865 (1987).
36. Pirajno, F., Grey, K. Chert in the Palaeoproterozoic Bartle Member, Killara Formation, Yerrida Basin, Western Australia: a rift-related playa lake and thermal spring environment? Precambrian Res. 113, 169-192 (2002).
37. Jackson, M.J., Muir, M.D., Plumb, K. A. Geology of the southern McArthur Basin. Bur. Miner. Resour. Geol. Geophys. Bull. Aust. 220, 173 (1987).

Acknowledgements: We thank Guoneng Chen, Qishun Fan, Qingkuan Li and Yongsheng Du for collecting data and discussing about data processing. ZJQ acknowledges support of the West Light Foundation of Chinese Academy of Sciences (Grant to Zhanjie Qin), Thousand Talents Plan of Qinghai Province (Grant to Zhanjie Qin), and the Second Tibetan Plateau Scientific Expedition and Research Program (STEP), Grant No. 2019QZKK0805. CAT acknowledges support of the Talent Cultivation Plan of "Xinghai Scholars" of Dalian University of Technology.

Author contribution: C.A. and Z.J. designed the study and wrote the manuscript. T.T., X.J., Y.S. and X.Y. assisted in the data collection and diagrams drawing. T.T., Z. and L.T. collated references. All authors contributed to data analysis and discussions and helped improve the manuscript.

Competing interests: The authors declare no competing interests.

Figures

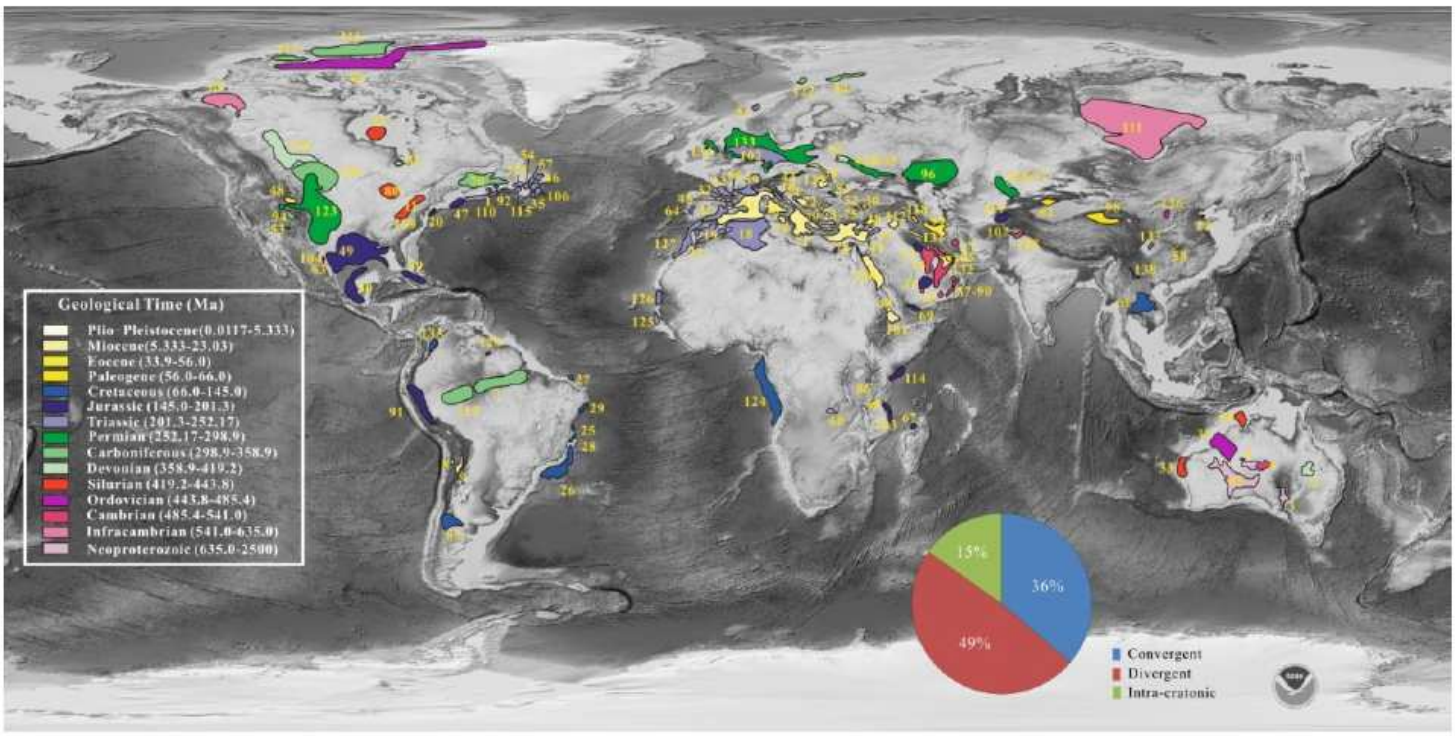

Figure 1

Distribution of evaporitic basins around the world through geological time (redrawn from1,25) (Extended Data Table 1). Basin names: 1. Abenaki (N. Scotian), 2. Adavale, 3. Adelaide Fold Belt, 4. Adriatic-Albanian Foredeep, 5. Amadeus Basin, 6. Amadeus Basin (Chandler), 7. Amazonas, 8. Andean, 9. Andean, 10. Apennine, 11. Appalachian, 12. Aquitaine, 13. Arabian Basin (Gotnia Salt Basin), 14. Arabian Basin (Hith Salt Basin), 15. Arabian Basin (Hormuz central Saudi Arabia), 16. Arabian Basin (Hormuz Gulf region), 17. Arabian Basin (Hormuz-Kerman region), 18. Atlas (Algerian-Tunisian), 19. Atlas (Moroccan), 20. Baltimore Canyon, 21. Berrechid, 22. Betic-Guadalquivir Basin, 23. Bohai Basin, 24. Bonaparte (Petrel), 25. Brazilian Aptian Basin (Camamu), 26. Brazilian Aptian Basin (Campos-Santos), 27. Brazilian Aptian Basin (Ceara), 28. Brazilian Aptian Basin (Cumuruxatiba), 29. Brazilian Aptian Basin (Sergipe-Alagoas), 30. Cankiri-Corum, 31. Canning Basin, 32. Cantabrian-West Pyrenees, 33. Carnarvon Basin (Yaringa), 34. Carpathian foredeep, 35. Carson Basin (Grand Banks), 36. Chu-Sarysu (Devonian), 37. Chu-Sarysu (Permian), 38. Cicilia-Latakia, 39. Cuban, 40. Danakil, 41. Dead Sea, 42. Dniepr-Donets, 43. Dniepr-Donets, 44. Eastern Alps, 45. Ebro Basin, 46. Flemish Pass Basin (Grand Banks), 47. Georges Bank, 48. Green River Basin, 49. Gulf of Mexico (northern Gulf coast), 50. Gulf of Mexico (southern; Salina-Sigsbee), 51. Haltenbanken, 52. Haymana-Polatli, 53. Holbrook Basin, 54. Horseshoe Basin (Grand Banks), 55. Hudson Bay, 56. Ionian, 57. Jeanne d' Arc Basin (Grand Banks), 58. Jianghan Basin, 59. Jura/Rhodanian, 60. Katangan, 61. Khorat Basin, 62. Kuqaforeland (Tarim Basin), 63. La Popa (Monterrey) Basin, 64. Lusitanian, 65. Mackenzie Basin, 66. Maestrat, 67. Majunga Basin, 68. Mandawa Basin, 69. Ma' Rib-Al Jawf/Shabwah (Hadramaut), 70. Maritimes Basin, 71. Mediterranean-Western, 72. Mediterranean-

Adriatic, 73. Mediterranean-Andros Basin, 74. Mediterranean-Cretean Basin, 75. Mediterranean-Samothraki basin, 76. Mediterranean-Tyrrhenian, 77. Mediterranean-Central, 78. Mediterranean-Eastern, 79. Mediterranean-Sicilian, 80. Michigan Basin, 81. Moesian, 82. Moose River Basin, 83. Neuquen Basin, 84. Nordkapp Basin, 85. Officer Basin, 86. Olduvai depression, 87. Oman (Fahud Salt Basin), 88. Oman (Ghaba Salt Basin), 89. Oman (Ghudun Salt Basin), 90. Oman (South Oman Salt Basin), 91. Oriente-Ucayali (Pucara) Basin, 92. Orpheus Graben, 93. Palmyra, 94. Paradox Basin, 95. Parry Island Fold Belt, 96. Pricaspian Basin, 97. Pripyat Basin, 98. Qaidam Basin, 99. Qom-Kalut, 100. Red Sea (north), 101. Red Sea (south), 102. Rot Salt Basin, 103. Ruvuma Basin, 104. Sabinas Basin, 105. Sachun Basin, 106. Salar Basin (Grand Banks), 107. Salt Range (Hormuz-Punjab region), 108. Salt Range (Kohat Plateau), 109. Saltville (Appalachian), 110. Scotian Basin, 111. Siberia, East, 112. Sirjan Trough,113. Solimoes, 114. Somalia-Kenya, 115. South Whale Basin (Grand Banks), 116. Sverdrup Basin (EllefRingnes-NW Ellesmere), 117. Sverdrup Basin (Melville Is.), 118. Tabriz Salt Basin, 119. Tadjik Basin, 120. Takutu Salt Basin, 121. Transylvanian, 122. Tromso Basin, 123. USA Midcontinent, 124. West Africa (Angola-Gabon), 125. West Africa (Gambia-Guine Bissau), 126. West Africa (Mauritania-Senegal), 127. West Africa (Morocco-S.Spain), 128. Western Canada (Alberta Basin), 129. Whale Basin (Grand Banks), 130. Williston Basin, 131. Zagros (Mesopotamian Basin), 132. Zagros (Mesopotamian Basin), 133. Zechstein (NW Europe), 134. Zechstein (onshore UK), 135. Zipaquira Basin, 136. Erdos Basin, 137. Sichuan Basin, 138. Lanping-Simao Basin. Note: The designations employed and the presentation of the material on this map do not imply the expression of any opinion whatsoever on the part of Research Square concerning the legal status of any country, territory, city or area or of its authorities, or concerning the delimitation of its frontiers or boundaries. This map has been provided by the authors.

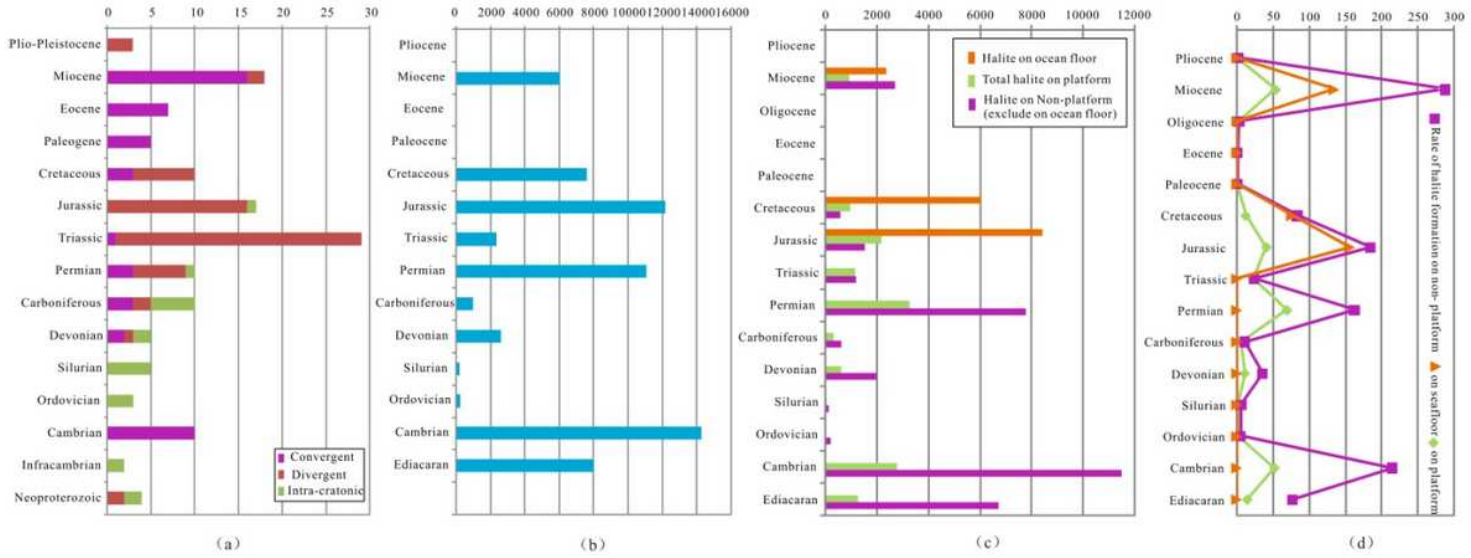

Figure 2

The relationship between mass of evaporate and tectonics in the geological time. a, Distribution of different tectonic types of evaporitic basins through geological time (data from1). b, Total masses of halite in different geological periods(mass×1015 kg).c, Masses of halite in different tectonic types of

evaporitic basins through geological time (mass×1015 kg). d, Rates of salt formation in different tectonic types of evaporitic basins through geological time (1015 kg/Ma); (data are from12, 26, 27).

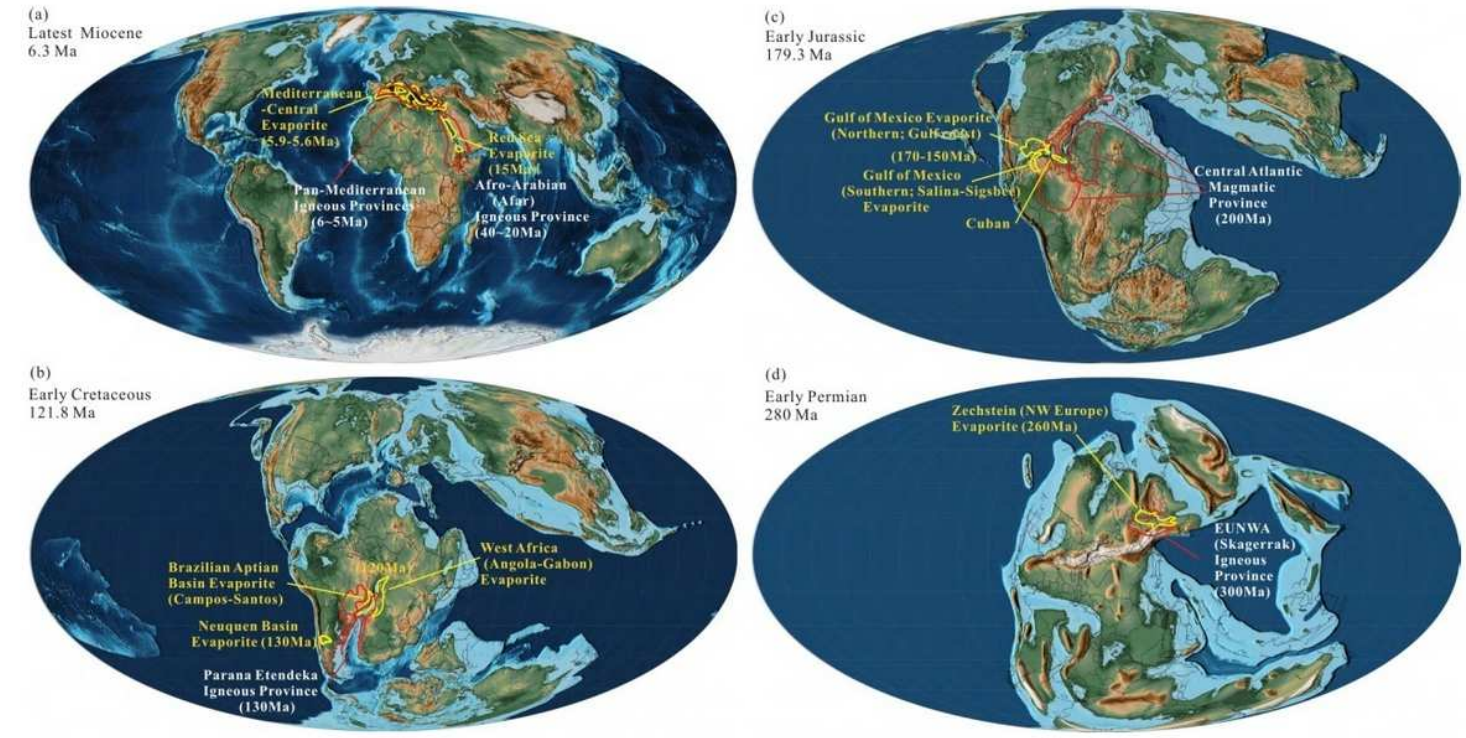

Figure 3

Comparisons between Large Igneous Provinces (LIPs) (data are from18), and Large Evaporite Provinces (LEPs) (data are from12,26,27) in different tectonic settings through the geological time (data are from28,29). a-d show the corresponding relationships of locations and ages. a. The Pan-Mediterranean igneous province and the Mediterranean evaporite, and the Afro-Arabian igneous province and the Red Sea evaporite in the Miocene; b. the Parana Etendeka igneous province and the South Atlantic evaporite in the Cretaceous; c. the Central Atlantic Magmatic Province and the Gulf of Mexico evaporite in the Jurassic; d. the Eunwa igneous province and the Zechstein evaporite in the Permian. Note: The designations employed and the presentation of the material on this map do not imply the expression of any opinion whatsoever on the part of Research Square concerning the legal status of any country, territory, city or area or of its authorities, or concerning the delimitation of its frontiers or boundaries. This map has been provided by the authors.

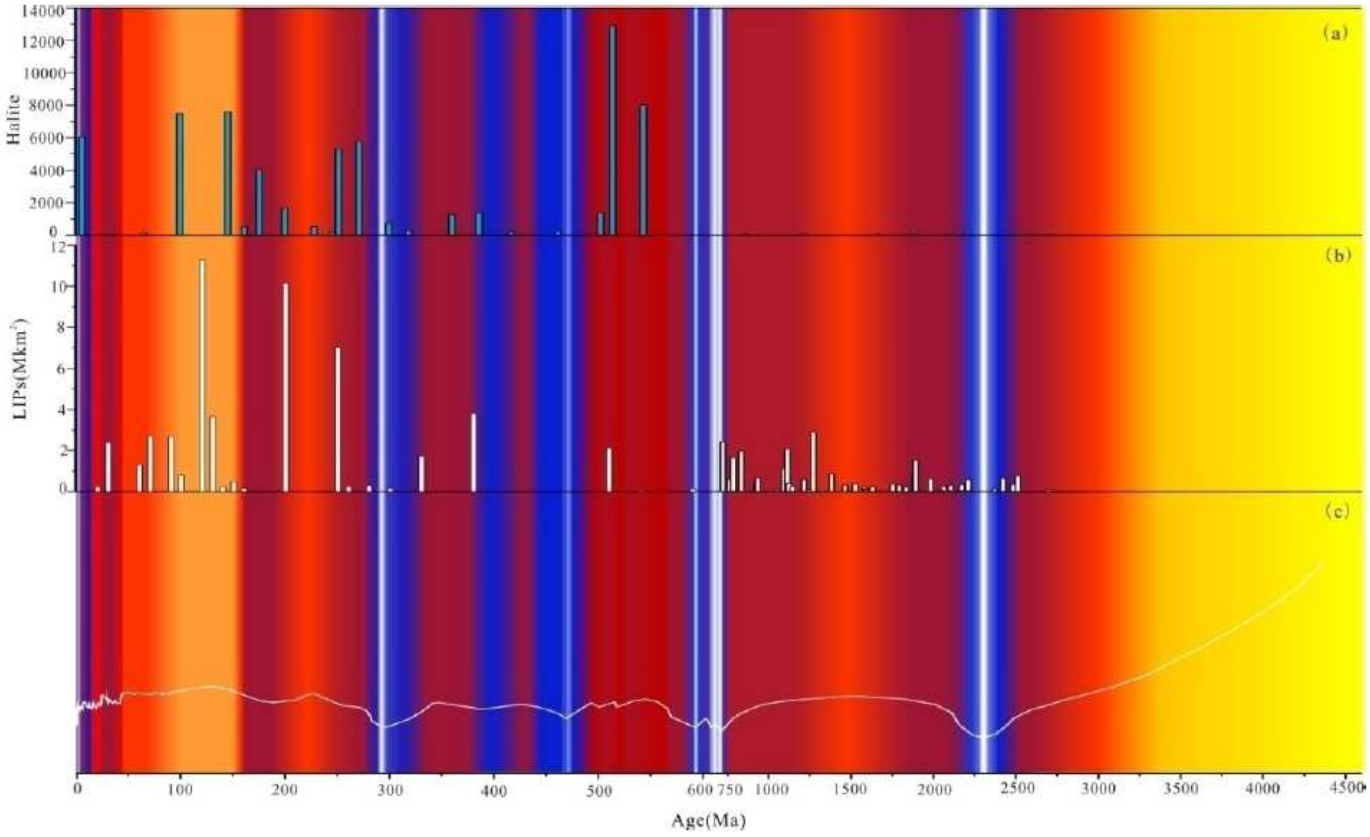

Figure 4

The corresponding relationships among evaporate (halite), Large igneous provinces (LIPs) and Thermal cycle in the geological time (the colour in the figure indicates the relative temperature of Earth's surface layer, with yellow, red, blue and white representing temperature from warm to cool, respectively). a, Temporal distribution of masses of evaporites (redrawn from12, 26, 27, 31-37). b, Temporal distribution of area of the large igneous provinces (redrawn from1, 18). c, Schematic diagram of the global thermal cycle in Earth evolution (redrawn from23).

Supplementary Files

This is a list of supplementary files associated with this preprint. Click to download.

- ExtendedDataTables.pdf